UNIVERSITY OF NEW MEXICO
ALBUQUERQUE

ENGINEERING EXPERIMENT STATION

N64-19850

CODE-1
NASA CR-53850 *

AN INVESTIGATION OF ELECTRICAL CHARACTERISTICS
OF THE LUNAR SURFACE

STATUS REPORT FOR PERIOD
1 November 1962 to 31 October 1963

Technical Report
EE-104

by

Nasir Ahmed
James A. Doran
Ahmed Erteza
Donald H. Lenhart

OTS PRICE

XEROX $

MICROFILM $

1812692

UNIVERSITY OF NEW MEXICO
ENGINEERING EXPERIMENT STATION
Albuquerque, New Mexico *U., Albuquerque*

t: AN INVESTIGATION OF ELECTRICAL CHARACTERISTICS
OF THE LUNAR SURFACE

STATUS REPORT, ~~FOR PERIOD~~
1 November 1962 ~~to~~ 31 October 1963

Technical Report EE-104

by
Nasir Ahmed,
James A. Doran,
Ahmed Erteza, *and*
Donald H. Lenhert *Mar. 1964*   *34p*

March, 1964

(NASA CR-53880; ~~Tech. Rept~~; EE-104) OTS: $ -- See Cover

CONTENTS

PART I
SUMMARY OF WORK ACCOMPLISHED

1.0 Introduction

The research work accomplished under NASA grant NsG 129-61, for the period November , 1962 to October , 1963, may be divided into the following categories:

1) Correlation of radar and photographic data.

2) Literature search and preliminary calculations to estimate dielectric properties of the surface of the moon.

3) Methods of determining an improved estimate of lunar surface roughness and electromagnetic properties.

2.0 Correlation of Radar and Photographic Data

This work describes an approach to the study of correlation between pulsed radar and photographic data as a method of supplementing the available statistical information on area-extensive radar scattering surfaces. A measure of the scattered energy is obtained by studying the variance and power spectra of the radar and photographic data. These spectra are obtained by taking the Fourier transform of the respective autocorrelation functions obtained from the radar and photographic data. Therefore, the variance and power spectra are considered for correlation studies.

There is a strong correlation between the radar and photographic variance and power spectra for farmland. There is a relatively weak correlation for the spectra obtained from residential and industrial areas. Therefore, the results seem to indicate that correlation between the radar and photographic data depends on the nature of the terrain. However, it is felt that

in order to make any definite statement regarding the extent to which the correlation of these spectra depends on the type of terrain, further investigations are necessary.

This work has been reported on in the UNM Technical Report EE-89, May, 1963.

3.0 Literature Search

This bibliography is the result of a literature search made during our research on National Aeronautics and Space Administration Grant NsG 129-61. Several different major topic areas are included in this bibliography.

These areas are:

1) Backscatter and Radar Return.

2) Lunar Surface Properties.

3) Acoustic Instrumentation and Simulation of Radar Return from Terrain and Geometrical Shapes.

4) Correlation of Radar and Photographic Data.

The list of references which resulted from this research and the associated literature searches is compiled to make available to others working in these fields a starting point for their own literature searches.

This work has been reported in UNM Technical Report EE-92, June, 1963.

4.0 Methods of Determining an Improved Estimate of Lunar Surface Properties

In reviewing radar return data taken from a variety of

terrestrial surfaces, it was noted that the initial rise of the pulse was, in general, linear with time. The probability densities of the initial slope was obtained for three different terrains (See Part II). The mean of the initial slopes indicates that it may be possible to differentiate between the surfaces and find their properties from the probability density of initial slopes and its mean.

The height distributions were also obtained for these three surfaces, but these results appear unrealistic as indicated in Part II, Section 4.0.

The majority of our future work will be directed toward the theoretical justification of the linear initial slope and in establishing the significance of its mean, if any.

5.0 Acoustic Simulator

Work has been accomplished on the electronics for the receiving system in the acoustic simulator in preparation for experiments to determine the effect of roughness. This work consisted of design, fabrication and check out of two time gates in order to allow more automatic and easier reduction of data taken in the simulator. This work has decreased toward the end of the reporting period to allow for more theoretical work to be accomplished prior to the running of experiments. This theoretical work will provide the basis for such future experiments.

---

[1]As of March, 1964, this theory is being prepared into a paper for submission to Radio Science-Journal of Research NBS/USNC-URSI-Section D.

6.0 Depolarization Experiment

Attempts were made to analyze the data taken in the depolarization experiment reported previously.[2] These attempts failed to obtain a solution due to the complexity of the problem involving spherical waves rather than plane waves incident on the target. This work was discontinued for the present in order to accomplish more theoretical study on the areas pointed out in Part I, Section 4.0 and Part II, with the anticipations that the results of that work could be extended to polarization and materially aid the data reduction of the polarization experiment.

7.0 Other Work

No work has been accomplished on the Aerobee High Altitude Radar experiment as no data has been obtained on these firings.

8.0 Future Research

The majority of our future research will be directed toward the theoretical justification of linear slope philosophy. The first area of investigation will be the slope of the return pulse for smooth geometrical bodies.[3] The following areas will be investigated after the first area has been solved.

1) Effect of roughness.

---

[2]Lenhert, D. H. and W.W. Koepsel,"Lunar Surface Characteristics Based on Radar and Photographic Data," University of New Mexico Engineering Experiment Station Report PR-39, October, 1962.

[3]This work is presently well under way. Portions of this work have been completed (See footnote 1).

2) Effect of transients.

3) Effect of polarization.

9.0 Travel

No trips were made by the research personnel during this period.

PART II
INITIAL SLOPE THEORY

1.0 Introduction

It is desired to obtain a quantitative description of
the surface roughness and reflectivity from the radar return
obtained from the surface of some planet such as the moon.
If there exists a method to obtain such parameters, it must
be able to stand the test directly when applied to radar
return data from known terrestrial targets. Once such a
method has been proven, then it may be applied to the analysis
of radar return data from the moon. This section is concerned
with such studies.

It has been observed that any radar return pulse has
a distinct linear slope beginning with the instant the return
becomes discernable. It is felt that the slope and extent
of time during which the slope remains linear are directly
related to the area dimensions, reflectivity, and surface
roughness. Radar data obtained from the moon also shows
a predominant log linear slope in the leading edge of the
returned pulse (see Fig. 1.1). Thus the techniques employed
to analyze terrain return data may be used to study the gross
features pertaining to the lunar surface and its average
dielectric constant. This requires that the slope theory
be verified using actual terrestrial terrain return data.
It will be necessary to develop a theory which is consistent
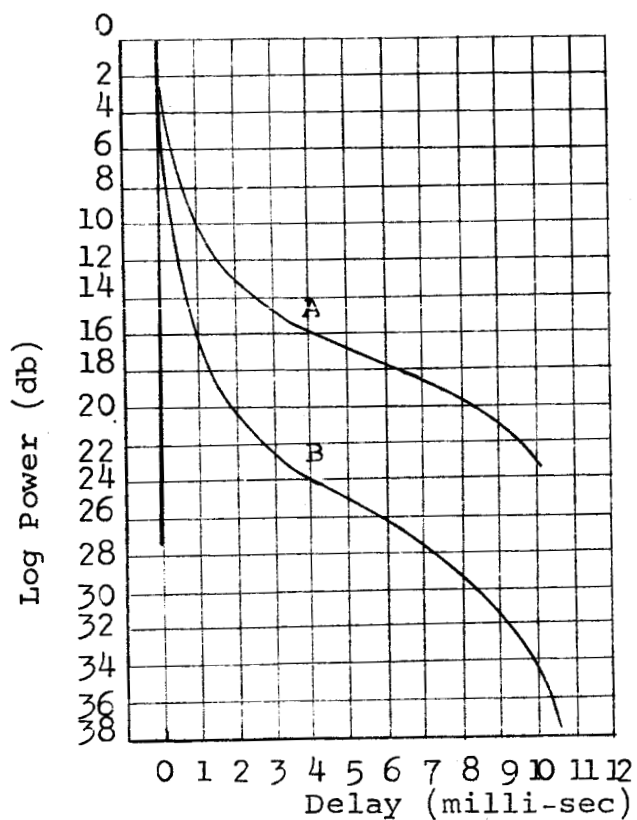
A: 3.6cm Wavelength 30 micro-sec. Transmitter Pulse.
B: Pettengill's Results 68cm Wavelength, 65 micro-sec Transmitter Pulse.[4]

Fig. 1.1 The Curve for Echo Intensity Plotted Against a Linear Range-Delay Axis.

_____

[4]Pettengill, G. H. and Henry, J. C.,"Radar Measurements of the Lunar Surface," Proceedings of the Lunar Symposium (No. 14 on the Moon), IAU, Leningrad (1960).

with the observations. However, it may be added that the
data to be used for verification purposes must have a reasonable
signal to noise ratio.

Another possible application of the slope theory has
been considered. This concerns the problem of classification
of terrains. It is believed that one may be able to classify
a terrain when its complex dielectric constant and the manner
in which its profile changes from pulse to pulse are known.
This change in the profile with reference to a datum is obtained
by considering the delay time corresponding to the leading
edge of the returned pulse.

In order to substantiate the slope theory and illustrate
its applications, radar data obtained from a water surface,
farmland and an industrial area have been investigated.
The results obtained from these investigations have been included
in this report.

2.0 Radar Data Available for Analysis

The data that has been used to substantiate the "slope
theory" was part of an experimental program to investigate
the reradiation properties of terrain at near-vertical
incidence. This program was initially carried out by the
Sandia Corporation.[5]

---

[5]Williams, C.S., Jr., Bidwell, C.H. and Gragg, D. M.
"Radar Return from the Vertical for Ground and Water Surfaces,"
SCR-107, April 1960.

The approximate characteristics of the radar used in obtaining the data are given in Table 2.1.

Table 2.1

	No.1	No. 2
Frequency	3800 m cps	415 mcps
Pulse Width	0.2 micro-sec	0.1 micro-sec
Antenna Gain	12 db	5 db

More detail concerning the pulse shapes and antenna patterns is given in Part III in Figs. III -1 through III-5 of the report concerned.

While obtaining the data, the radars were carried by a 130-knot aircraft that made straight and level runs, each of several seconds duration, over the individual terrains. The antennas were directed straight down. The effects of polarization of the transmitted wave were ignored.

Radar data obtained from a farmland, an industrial area and a water surface were considered for the purpose of analysis. Brief descriptions pertaining to these terrains will be given now. For more details one might refer to Sandia Corporation Technical Memorada (SCTM)[6].

1. <u>Farmland: Imperial Valley of California</u>

This terrain consists of a cultivated and irrigated farm-land covered with heavy growth of pasture and grasslike crops. The irrigation is sufficient to cause the ground to be rather wet. (SCTM 254-55-54) by R.K. Moore.

---

[6] Williams, <u>loc. cit.</u>

2.   <u>Industrial Area: St. Paul, Minnesota</u>

The terrain consists of factory buildings which are all very large and predominantly metal roofed. Some are constructed wholly of corrugated metal. Trees are scattered through the area but by no means predominant. Very little open ground exists in the area except for a few parking lots. (SCTM 57-55-54) by D. M.Gragg.

3.   <u>Water Surface: Lake Benidji, Minnesota</u>

This lake is located in the northern part of Minnesota. While obtaining data, the water was slightly ruffled by winds which caused approximately one foot waves. (SCTM 163-55-54) by D.M. Gragg.

3.0   <u>Procedure of Data Analysis and Results:</u>

Radar data obtained from a water surface, farmland and an industrial area have been analyzed with a view to obtaining the following terrain characteristics:

1. The probability density distribution of the slopes associated with the leading edge of the returned pulse during the linear portion.

2. The approximate terrain profile (with reference to some datum) obtained from considerations of the delay time corresponding to the leading edge of the returned pulse.

Now, the probability density distribution of slopes eventually yields the complex dielectric constant and hence the reflection coefficient of the terrain. Thus, in what follows, this will

be referred to as the probability density distribution of terrain surface reflectivity.

The film is read on a Recordak film reader. Fig. 3.1 represents the display of a typical returned pulse on the Recordak.
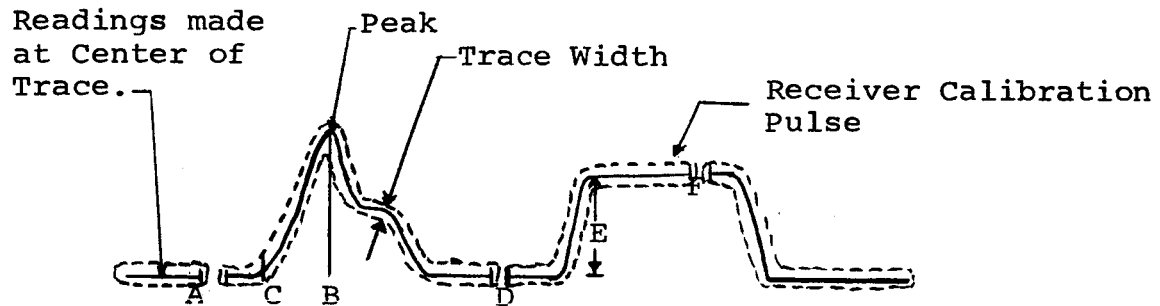
Radar data that has been obtained from the various types of terrains consist of about two thousand five hundred pulses. However, it is sufficient to consider the first five hundred of these to obtain the characteristics of interest mentioned above.

Details pertaining to the techniques employed to obtain these characteristics will now be considered.

3.1 The Probability Density Distribution of Surface Reflectivity:

In order to obtain the slope it is found more convenient to first measure the angle between the horizontal and the linear rise of the leading edge of each pulse. Then the trigonometric tangents of these angles yield the corresponding slopes. Thus, one may represent the angles so measured by θi (i=1,2,.....500).

While obtaining the angles θi° (i=1,2,.....500), an error of $\pm 1.5^{\circ}$ was assumed. Thus, the ensemble of the 500 pulses was divided into groups or classes with class intervals of 3°, so as to distribute the error incurred uniformly. The following statistics pertaining to the ensemble and these classes may now be defined:

Readings made
at Center of
Trace.⌐   ⌐Peak
                         ⌐Trace Width   Receiver Calibration
                                               Pulse

E

A   C   B   D

A= Reference Point for Measurement of Delay Time to
    Leading Edge of Pulse.

B= Point on Time Axis that Corresponds to the Peak
    Reading of Pulse.

C= Leading Edge of Pulse.

AD, DF= The Distance (time) between Time Markers.

E= Displacement of Calibration Pulse.

Fig. 3.1 A Typical Returned Pulse as Seen on the Recordak.

$\bar{\theta}$ = Mean value of the distribution.

$\bar{\theta}_k$ = Mid-value of the kth class, where, k=1,2,.....n and n is the total number of classes obtained from a given ensemble.

σ = The standard deviation of the distribution.

f_k = The class frequency of the kth class.

Thus, one may write:

$$\bar{\theta} = \frac{\sum\limits_{k=1}^{n} f_k \bar{\theta}_k}{\sum\limits_{k=1}^{n} f_k} \tag{3.1}$$

and,

$$\sigma = \sqrt{\text{Mean Value }(\bar{\theta}^2_k) - \bar{\theta}^2} = \sqrt{\frac{\sum\limits_{k=1}^{n} f_k \bar{\theta}_k^{\,2}}{\sum\limits_{k=1}^{n} f_k} - \bar{\theta}^2} \tag{3.2}$$

Again, from the class frequency f_k (k=1,2,.....n), it follows that:

P_k = The probability that the kth class will occur

$$= \frac{f_k}{\sum\limits_{k=1}^{n} f_k} \tag{3.3}$$

Thus, the desired probability distribution for the ensemble of the angles θi (i=1,2,.....500) may now be obtained by means of the statistics θ, σ, and P_k which have been defined in Eqs. 3.1, 3.2, and 3.3 respectively. Figure 3.2 shows a typical data reduction sheet which has been used to obtain the probability density distribution of terrain surface reflectivity. Such distributions that have been included in this report have been plotted

θ_i	f_i	$\bar{\theta}_i$	$\bar{\theta}_i^2$	P_i
7.5 – 10.5	1	9	81	.0008
9 – 12	1	10.5	110.25	.0008
10.5 – 13.5	1	12	144	.0008
19.5 – 22.5		21	441	0
21 – 24	2	22.5	506.25	.0016
22.5 – 25.5	2	24	576	.0016
24 – 27	2	25.5	650.25	.0016
25.5 – 28.5	4	27	729	.0033
27 – 30	3	28.5	812.25	.0025
28.5 – 31.5	4	30	900	.0033
30 – 33	5	31.5	992.25	.0042
31.5 – 34.5	5	33	1089	.0042
33 – 36	4	34.5	1190.25	.0033
34.5 – 37.5	5	36	1296	.0042
36 – 39	5	37.5	1406.25	.0042
37.5 – 40.5	6	39	1521	.0050
39 – 42	8	40.5	1640.25	.0067
40.5 – 43.5	13	42	1764	.0110
42 – 45	17	43.5	1892.25	.0143
43.5 – 46.5	24	45	2025	.0203
45 – 48	23	46.5	2162.25	.0194
46.5 – 49.5	20	48	2304	.0169
48 – 51	15	49.5	2450.25	.0127
49.5 – 52.5	10	51	2601	.0084
51 – 54	18	52.5	2756.25	.0152
52.5 – 55.5	19	54	2916	.0160
54 – 57	24	55.5	3080.25	.0203
55.5 – 58.5	25	57	3249	.0211
57 – 60	19	58.5	3422.25	.0160
58.5 – 61.5	25	60	3600	.0211
60 – 63	25	61.5	3782.25	.0211
61.5 – 64.5	40	63	3969	.0338
63 – 66	58	64.5	4160.25	.0491
64.5 – 67.5	62	66	4356	.0524
66 – 69	59	67.5	4556.25	.0499
67.5 – 70.5	61	69	4761	.0516
69 – 72	83	70.5	4970.25	.0702
70.5 – 73.5	74	72	5184	.0626
72 – 75	80	73.5	5402.25	.0677
73.5 – 76.5	79	75	5625	.0668
75 – 78	115	76.5	5852.25	.0973
76.5 – 79.5	85	78	6084	.0719
78 – 81	42	79.5	6320.25	.0355
79.5 – 82.5	8	81	6561	.0067
81 – 84	1	82.5	6806.25	.0008
82.5 – 85.5		84	7056	0

Right margin notes:

$\sum \bar{\theta}_i^2 = 774403$

$\sum f_i \bar{\theta}_i^2 = 5252157$

$\sum f_i \bar{\theta}_i^2 = 4447.2$; Thus $\sigma = 12.32$

$\sum f_i \bar{\theta}_i = 1181$; Thus $\bar{\theta} = 65.54°$

Fig. 3.2 Data Reduction Sheet

with respect to the normalized variable

$$\left[\frac{\bar{\theta}_k - \theta}{\sigma}\right] \quad ,$$

(See Figs. 3.3, 3.4, and 3.5). From these distributions, the
most probable angle and hence the most probable slope may be ob-
tained. In Fig. 3.1, the distance, AD, and the displacement of
calibration pulse E allow the sample means of the three probability
densities obtained to be referred to a fixed reference. The
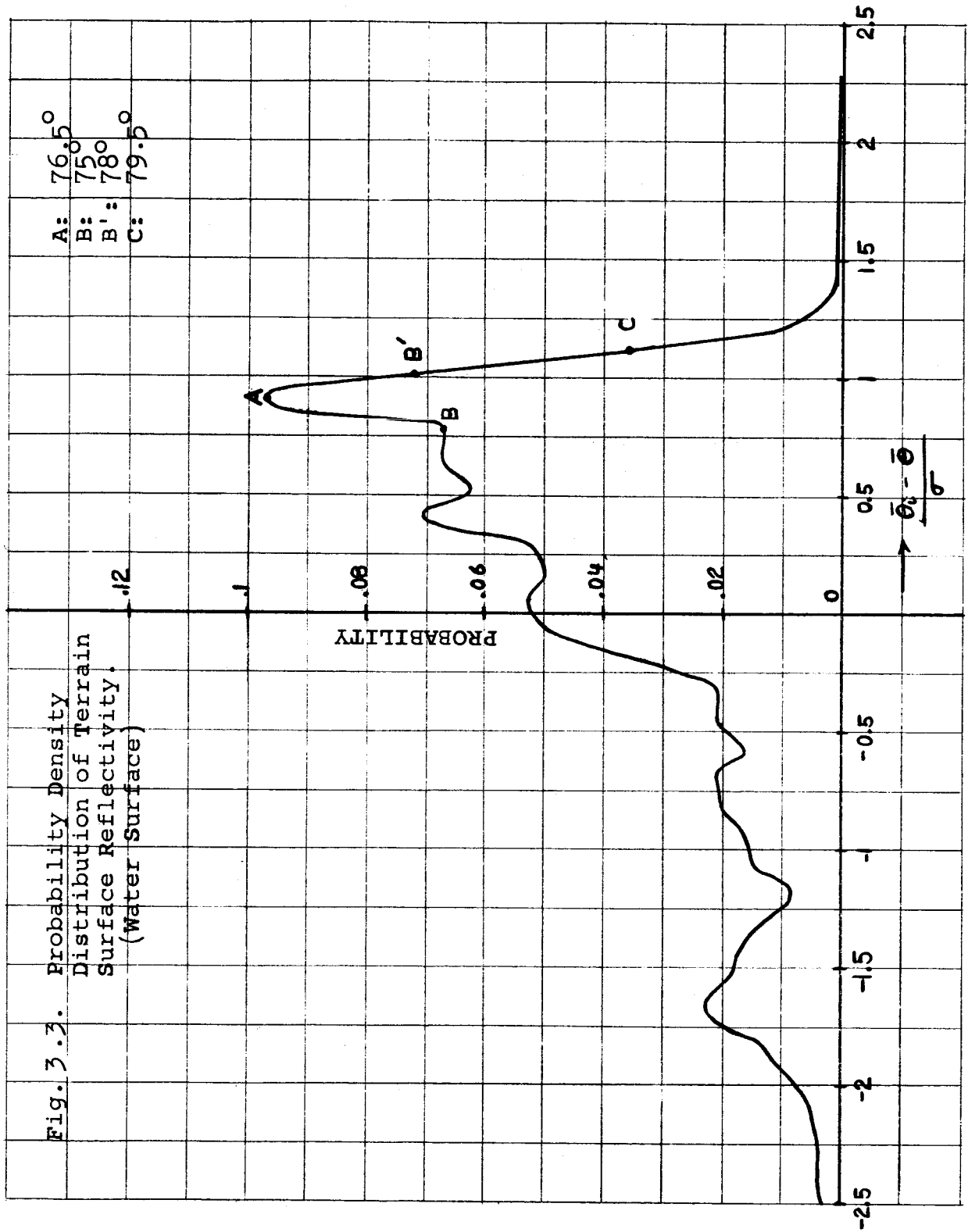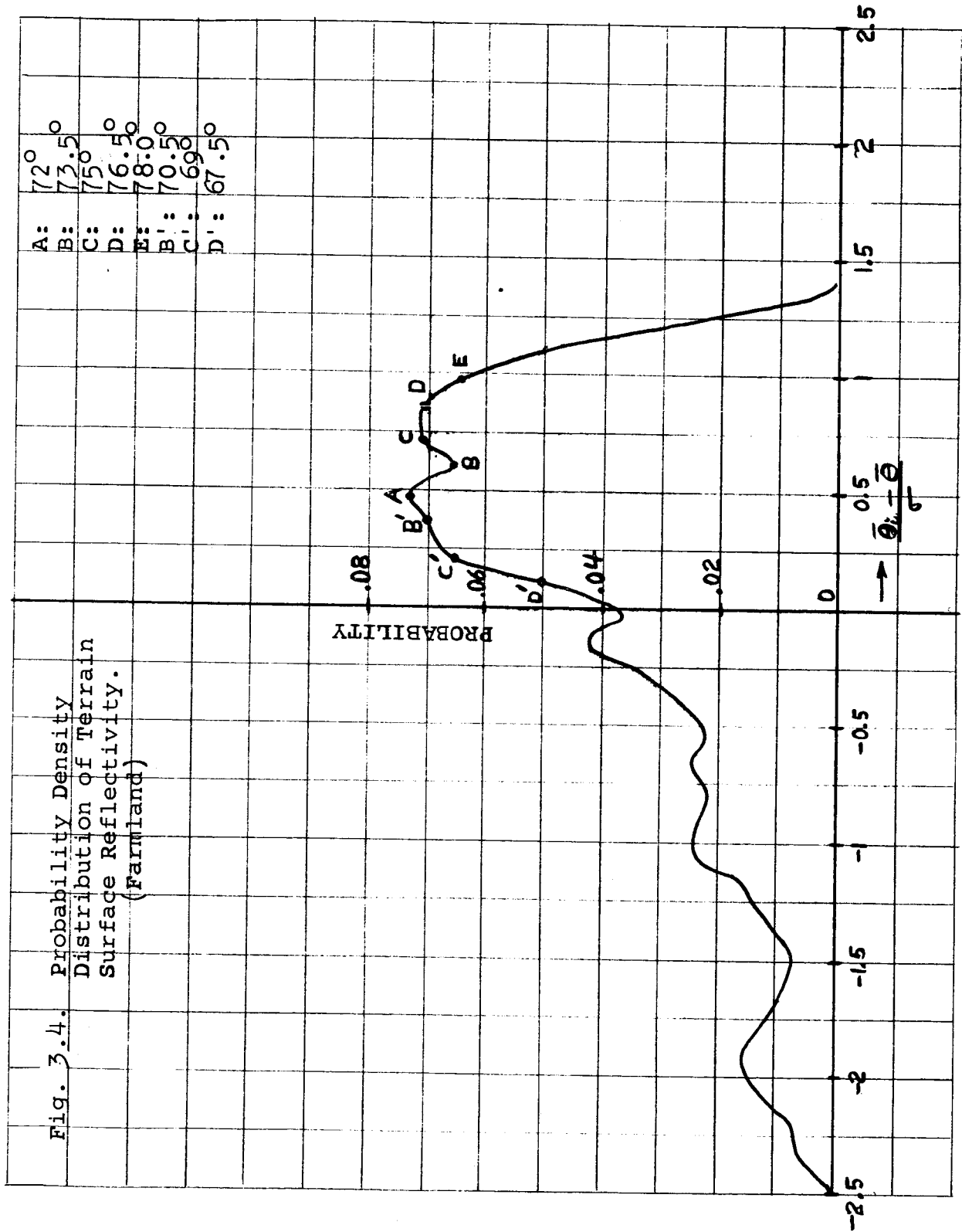sample means, $\bar{\theta}$, thus obtained are shown in Table 3.1.

<div align="center">Table 3.1</div>

Terrain Type	Mean Slope $\bar{\theta}$
Water Surface	12.5°
Farmland	14.4°
Industrial Area	27.4°

3.2 Terrain Profile:

To obtain the terrain profile it is required to measure the
delay time corresponding to the leading edge of the returned pulse
from a fixed reference point. In Fig. 3.1, a typical delay time
(in terms of an equivalent length) is represented by AC in centi-
meters. In general these delay times may be represented by t_i'
(i=1,2,.....500) where the prime indicates that the delay time
has been expressed in terms of an equivalent length in centi-
meters.

Now, the distances AD and DF (Fig. 3.1) each measure 11.75
cms. and it is known that these are equivalent to 1.991 micro-

Fig. 3.3. Probability Density Distribution of Terrain Surface Reflectivity. (Water Surface)

A: 76.5°
B: 75°
B': 78°
C: 79.5°

Fig. 3.4. Probability Density Distribution of Terrain Surface Reflectivity. (Farmland)

A: 72°
B: 73.5°
C: 75°
D: 76.5°
E: 78.0°
B': 70.5°
C': 69°
D': 67.5°

Fig. 3.5. Probability Density Distribution of Terrain Surface Reflectivity. (Industrial Area)

A: 79°
B: 77.5°
B': 80.5°
C: 82°
D: 76°
D': 83.5°
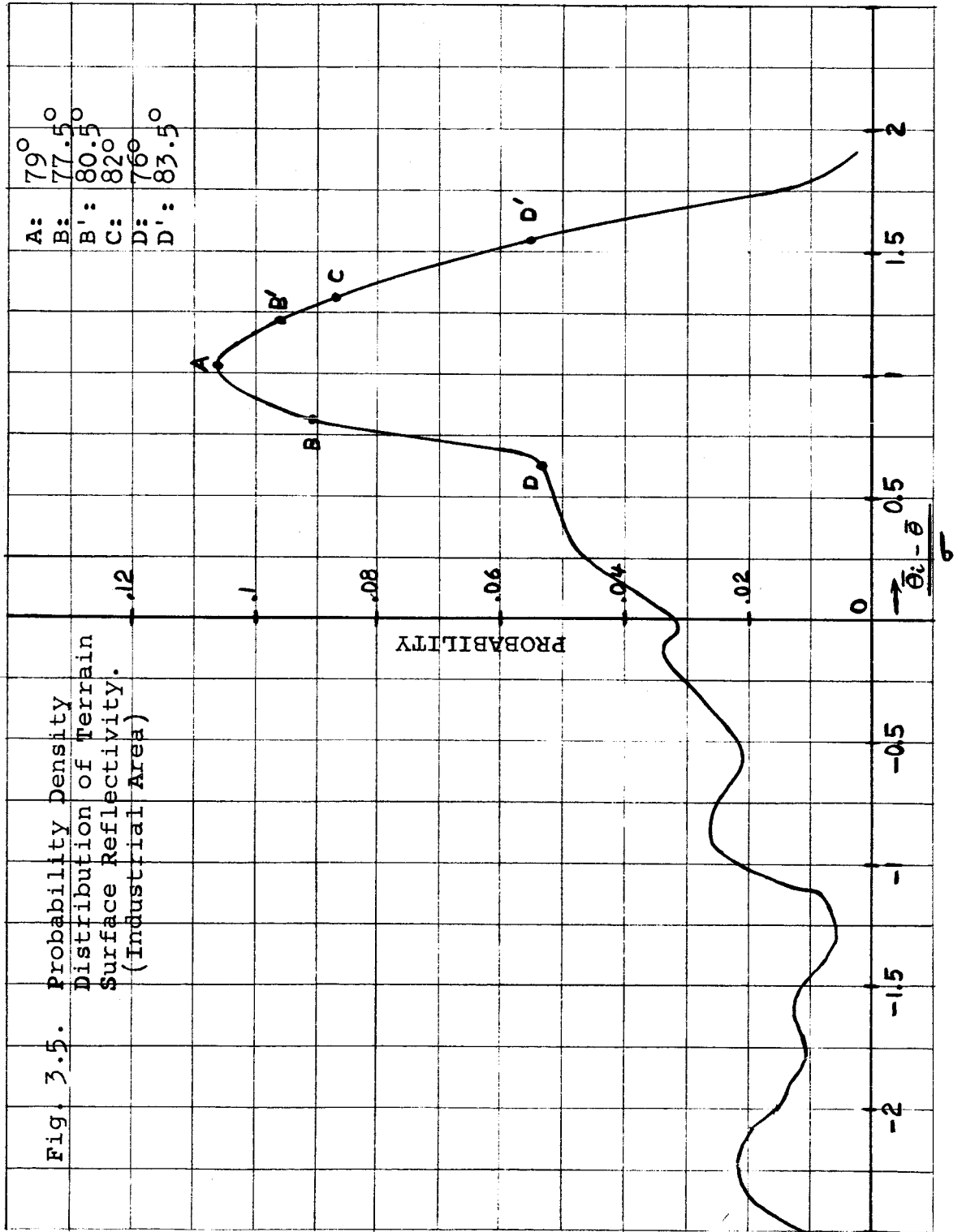
seconds with respect to time.[7] Thus, one has

$$1cm = 0.17017 \text{ micro-sec}$$

or   (3.4)

$$t_i cms = 0.17017 \; t'_i \text{ micro-sec} = t_i \text{ micro-sec}$$

Further, the velocity of propagation is 300 meters per micro-second or 984.42 feet per micro-second. Thus, from Eq. 3.4 it follows that,

$$1cm \text{ (As measured on the Recordak)} = 167.52 \text{ feet}$$
                                                                                      (3.5)

The mean delay time for the ensemble is given by

$$\bar{t}' = \frac{1}{500} \sum_{i=1}^{500} t'_i \tag{3.6}$$

Thus, from Eqs. 3.5 and 3.6 it follows that

$$h_i = \pm \frac{1}{2} \left[167.52 \; (t'_i - \bar{t}') \right] \text{ feet}$$

$$= \pm 83.76 \; (t'_i - \bar{t}') \text{ feet.} \tag{3.7}$$

where, h_i is the height of the terrain above or below a datun level corresponding to a t'_i as shown in Fig. 3.6.

Again, if the speed of the aircraft while obtaining radar

---

[7] Janza, F. J. "The Analysis of a Pulsed Radar Acquisition System and a Comparison of Analytical Models for Describing Land and Water Radar Return Phenomena," Sandia Corporation Monograph, SCR-533, January, 1963, pp. 72-73.

data is ν feet per second, then from Eq. 3.4 one has

$$d_i = 0.17017 \, \nu t'_i \text{ feet} \tag{3.8}$$

where d_i is the distance on the terrain along the line of flight of the aircraft. Terrain profiles that are included in this report have been plotted with respect to d as the variable, (See Figs. 3.7 and 3.8).
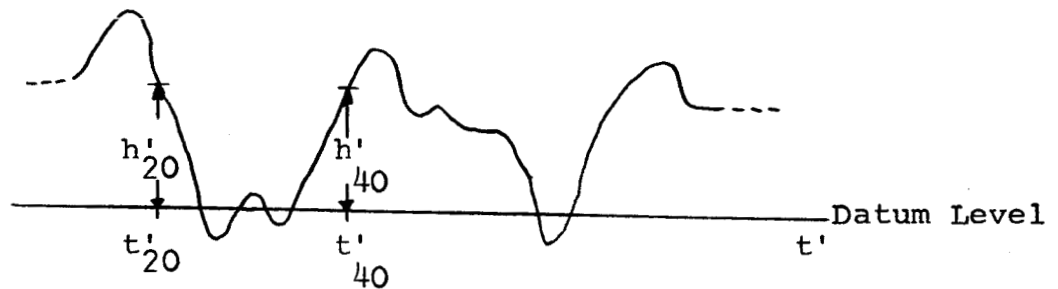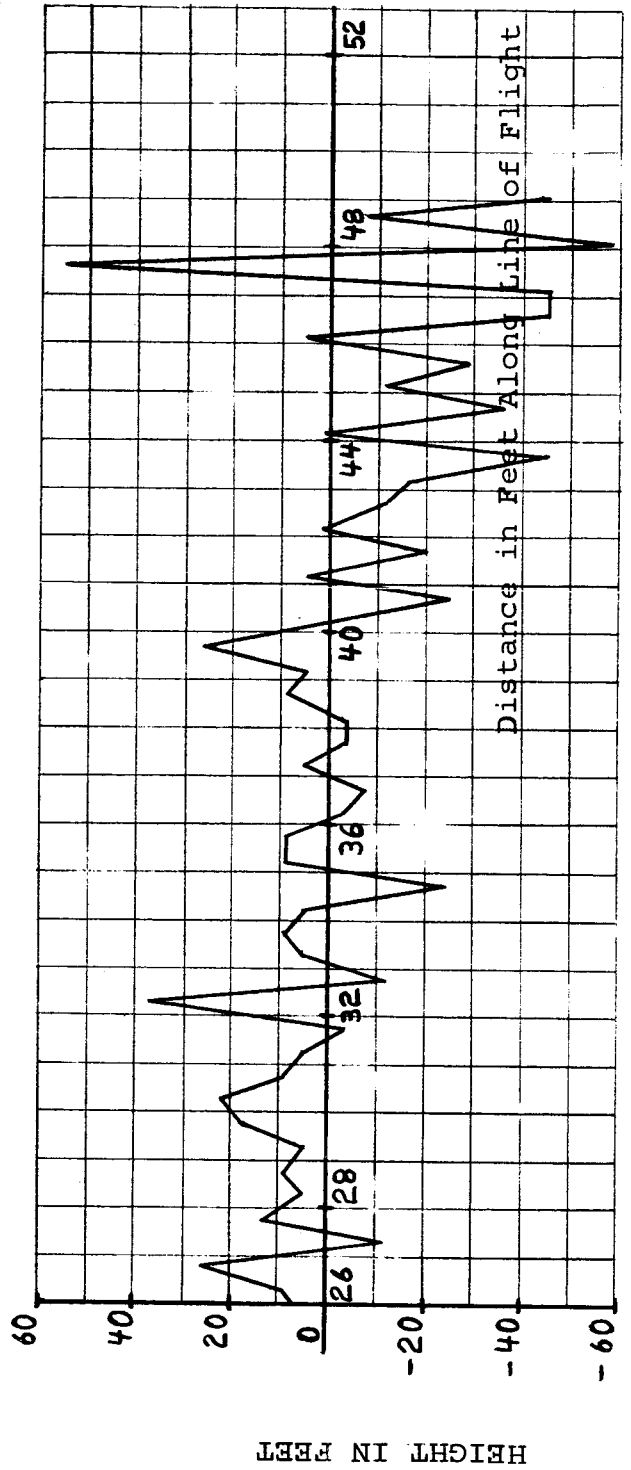

Fig. 3.6 A Representation of the Terrain
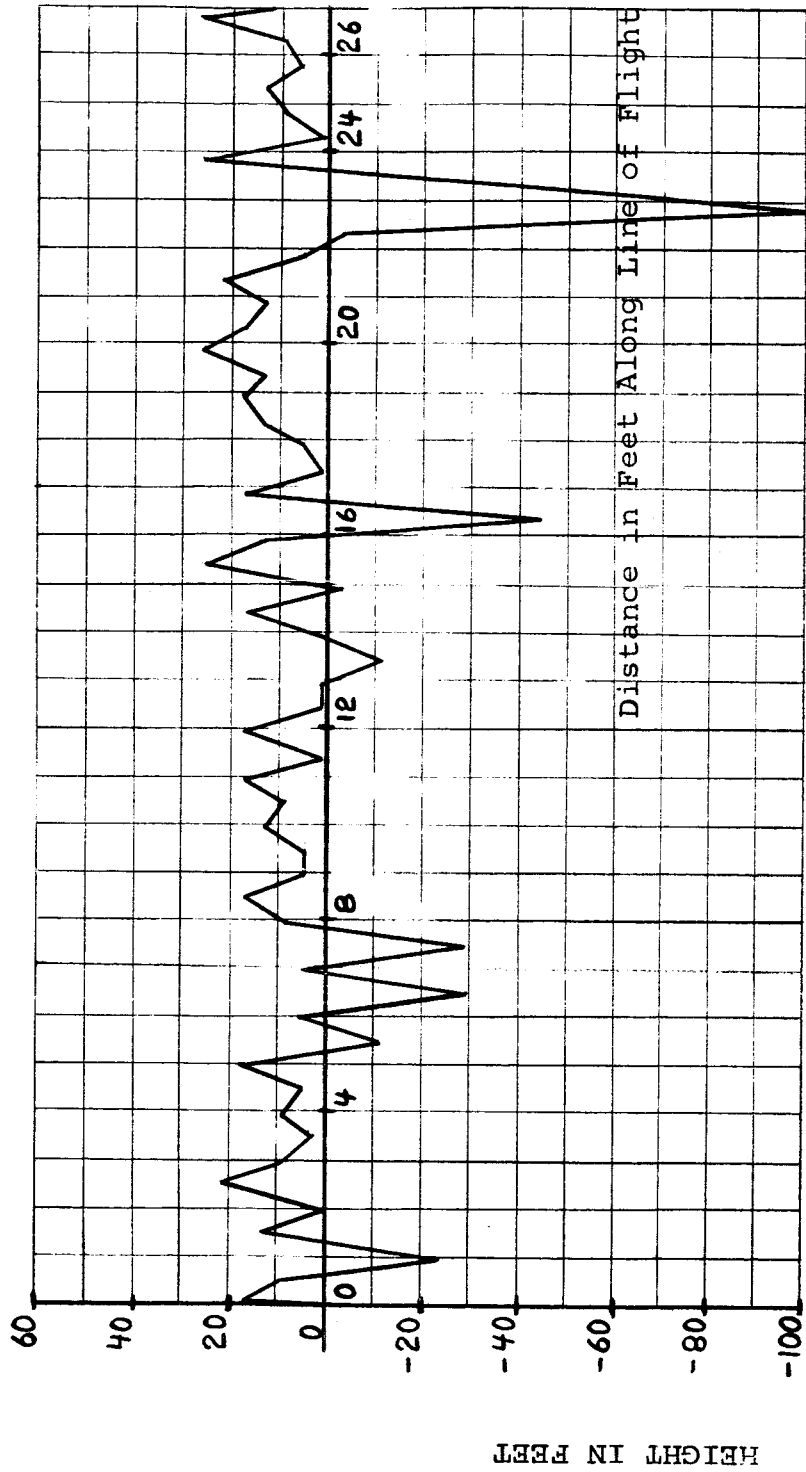Profile with Respect to the Variable t'_i.
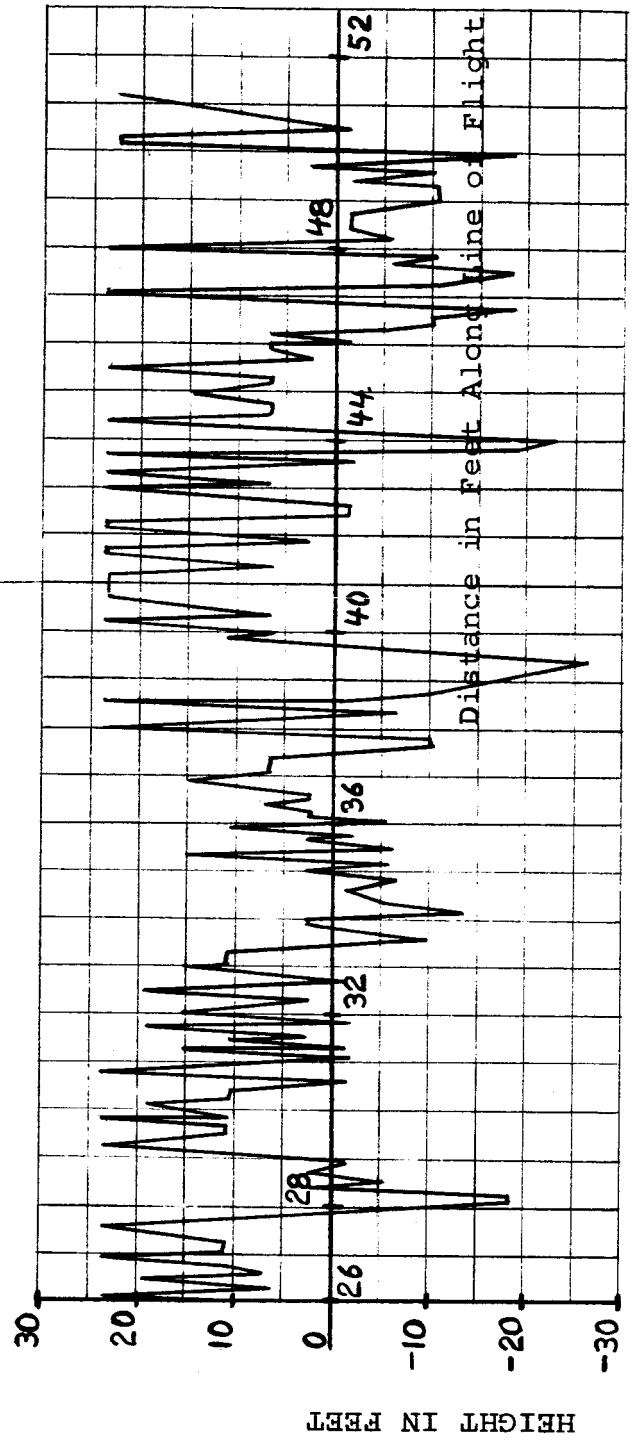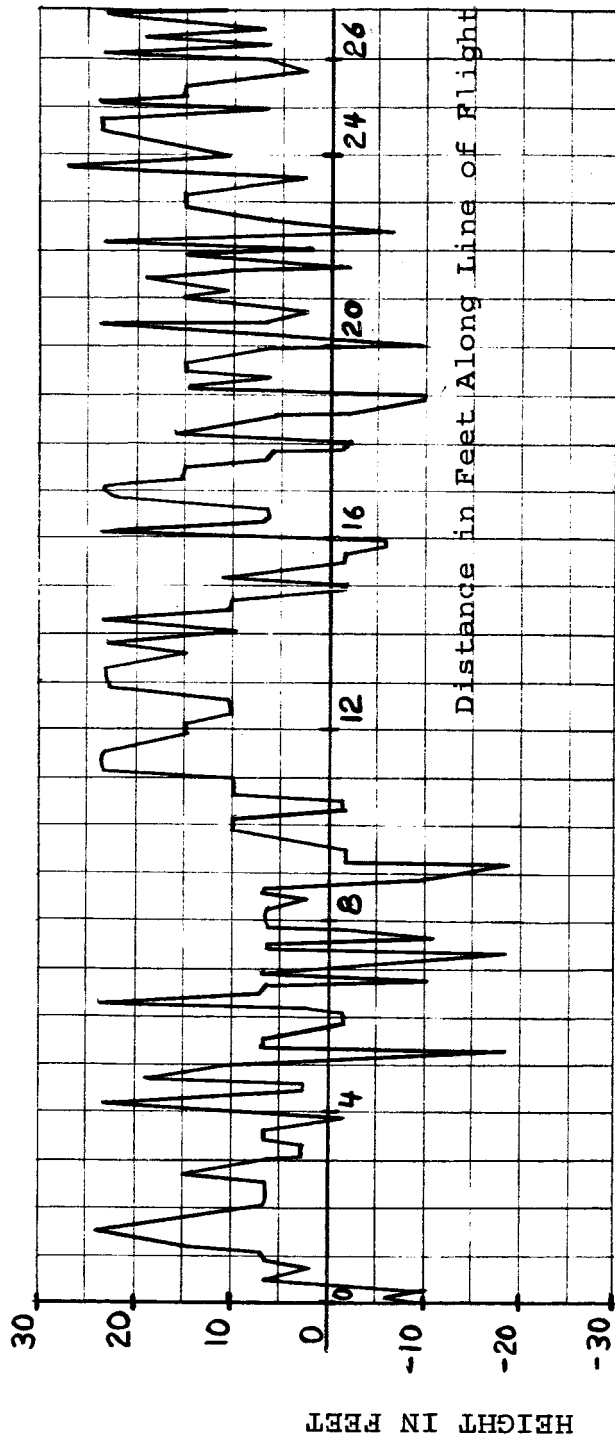
Fig. 3.7 TERRAIN PROFILE (INDUSTRIAL AREA)

Fig. 3.8   TERRAIN PROFILE (FARMLAND)

4.0 Conclusions:

The three mean slopes given in Table 3.1, while not absolute values of mean angle, indicated an ordering of the three surfaces. If a theoretical basis can be obtained for the mean slope, this would be a means of identifying the type of surface and/or the electromagnetic properties of the surface.

While the data obtained in Section 3.2 relating to the distribution of heights from an average surface are interesting, they do not appear to be realistic. A change of 40 feet elevation in 4 feet along the flight path does not appear to be realistic for farmland. This rapid change could be explained by using the linear slope. This time was measured with reference to the first discernable signal above the noise giving a threshold effect. Considering Figure 4.1, a change in slope without a change in height from the reference surface would give an indicated change in height.
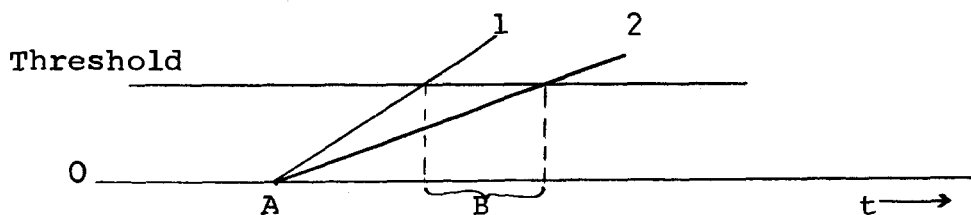
A = Time Corresponding to Actual Beginning of Rise.
B = Apparent Time Equivalent of Height Change Between (1) and (2) Due to the Different Slopes.

Fig. 4.1 Effect of Threshold on Indicated Height.

Therefore, unless a correlation function is used between slope of
return pulse and height this data has no significance.

The data obtained above indicated that the mean slope is
different for different surfaces. Consequently the majority of
our future work will be applied to obtaining a theoretical basis
for such differentiation between surfaces. The approach to this
problem will be to first study the return of plane and spherical
waves from a smooth body (i.e. geometrically describable surface)
and concentrate on the initial rise of the return. It is anti-
cipated that the smooth surface part of the problem will show
no polarization effect. Certain describable roughness will have
to be attributed to the smoth surface to bring about depolarization
in the return.

Computation of Reflection Coefficient ($|\rho|$) at 415 mcps

and 3800 mcps

It is desired to compute the theoretical curves of reflection coefficient ($|\rho|$) versus conductivity (σ) for various values of dielectric constant (ϵ). The values of the dielectric constants chosen are in the vicinity of those pertaining to a water surface (inorganic water), farmland and an industrial area. These curves may be used to good advantage to readily obtain $|\rho|$ for a given σ.

Fundamental transmission line concepts are employed to compute $|\rho|$. (See Fig. A.1). Accordingly one has,

$$\overline{\rho} = \frac{\overline{Z}_m - \overline{Z}_a}{\overline{Z}_m + \overline{Z}_a} \tag{A.1}$$

where,

$\overline{Z}_a$ = The air-terrain interface impedance "looking" from

region 1 into region 2.

$\overline{Z}_m$ = The air-terrain interface impedance "looking" from

region 2 into region 1.

Further,

$$\overline{Z}_a = \sqrt{\frac{\mu_o}{\epsilon_o}}$$

and

$$\overline{Z}_m = \sqrt{\frac{j\omega\mu_m}{\sigma_m + j\omega\epsilon_m}} \tag{A.2}$$

-25-

where,

μ_o = permeability of air = 1.257×10^{-6} henry/meter,

ϵ_o = permittivity of air = 8.854×10^{-12} farad/meter,

μ_m = permeability of medium,

ϵ_m = permittivity of medium,

ω = angular radian frequency = $2\pi f$, and

σ_m = conductivity of medium.

Thus from Eqs. A.2 one obtains

$$\bar{Z}_a = R_o = 377 \text{ ohms} \qquad (A.3)$$

and

$$\bar{Z}_m = \sqrt{\frac{\mu_m}{\epsilon_m}} \left[1 + \left(\frac{\sigma_m}{\omega\epsilon_m}\right)^2 \right]^{-1/4} \underline{/\theta} \qquad (A.4)$$

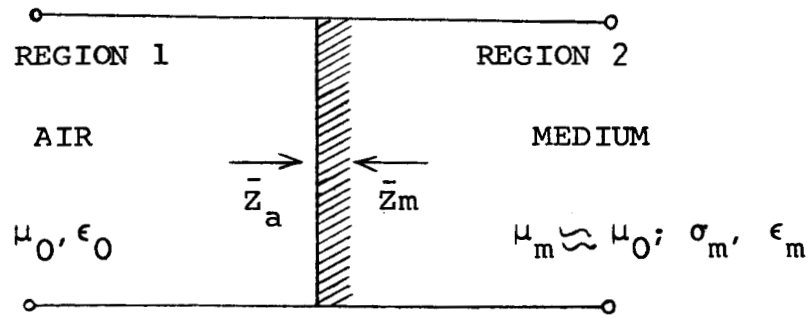On assuming that $\mu_m = \mu_o$ Eq. A.4 may be written as:

$$\bar{Z}_m = \sqrt{\frac{\mu_o}{\epsilon_m}} \left[1 + \left(\frac{\sigma_m}{\omega\epsilon_m}\right)^2 \right]^{-1/4} \underline{/\theta} = x + jy \qquad (A.5)$$

where,

$$x = \sqrt{\frac{\mu_o}{\epsilon_m}} \left[1 + \left(\frac{\sigma_m}{\omega\epsilon_m}\right)^2 \right]^{-1/4} \cos\theta$$

and

$$y = \sqrt{\frac{\mu_o}{\epsilon_m}} \left[1 + \left(\frac{\sigma_m}{\omega\epsilon_m}\right)^2 \right]^{-1/4} \sin\theta$$

$\bar{Z}_a$ = Air-terrain interface impedance "looking" from region 1 into region 2.

$\bar{Z}_m$ = Air-terrain interface impedance "looking" from region 2 into region 1.

μ_0 = Permeability of air = 1.257×10^{-6} henry/meter

ϵ_0 = Permittivity of air = 8.854×10^{-12} farad/meter.

μ_m = Permeability of medium.

ϵ_m = Permittivity of medium.

σ_m = Conductivity of medium.

Fig. A.1. Representation of the air-terrain interface as a transmission line terminal impedance.

Thus, from Eq. A.1 it may be shown that

$$|\rho| = \frac{\sqrt{(x^2 + y^2 - R_o^2)^2 + 4y^2 R_o^2}}{(x + R_o)^2 + y^2} \tag{A.6}$$

Now from Eq. A.6 $|\rho|$ is computed for a given ϵ with σ_m as the variable. The characteristics so obtained at frequencies of 415 mcps and 3800 mcps are included in this section (See Figs. A.2 through A.5). The values of conductivity and dielectric constant of some of the common types of terrains are listed in Table A.1.[8]

Table A.1

Terrain	Conductivity (σ) (mhos/meter)	Dielectric Constant (Farads/meter)
1. Mineral water[9]	0.21	76
2. Sea water	4	80
3. Rich agricultural, low hills	0.01	15
4. Marshy, forested flat land	0.008	12
5. Pastoral land, medium hills and forestation	0.005	13
6. Mountainous (hills up to 3000 ft)	0.001	5
7. Cities, residential areas	0.002	5
8. Cities, industrial areas	0.0001	3

---

[8] International Telephone and Telegraph Corporation; Reference Data for Radio Engineers; American Book - Stratford Press Incorporated, N.Y.: Fourth Edition, p. 714.

[9] Janza, F. J. Op. cit. p. 106.

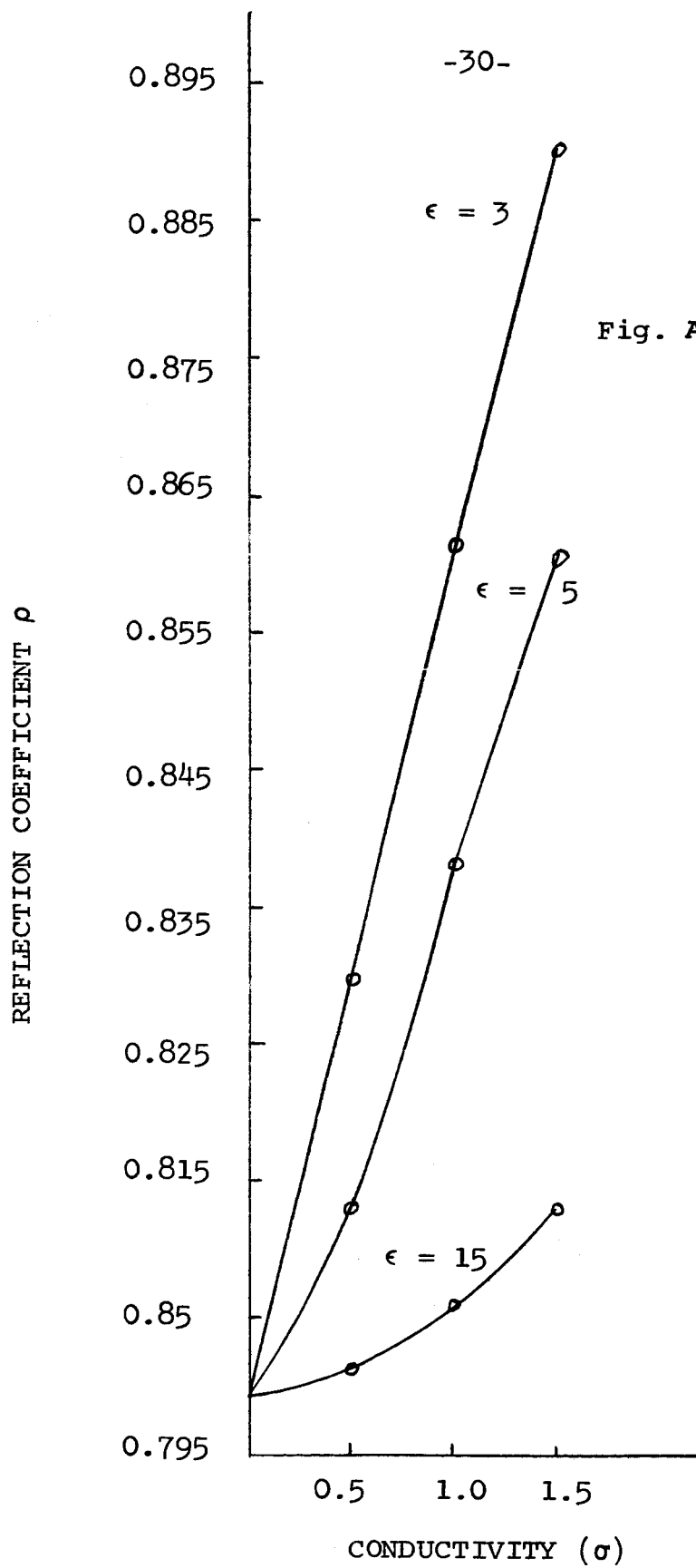Fig. A.2   Reflection Coefficient Versus
Conductivity Characteristics.
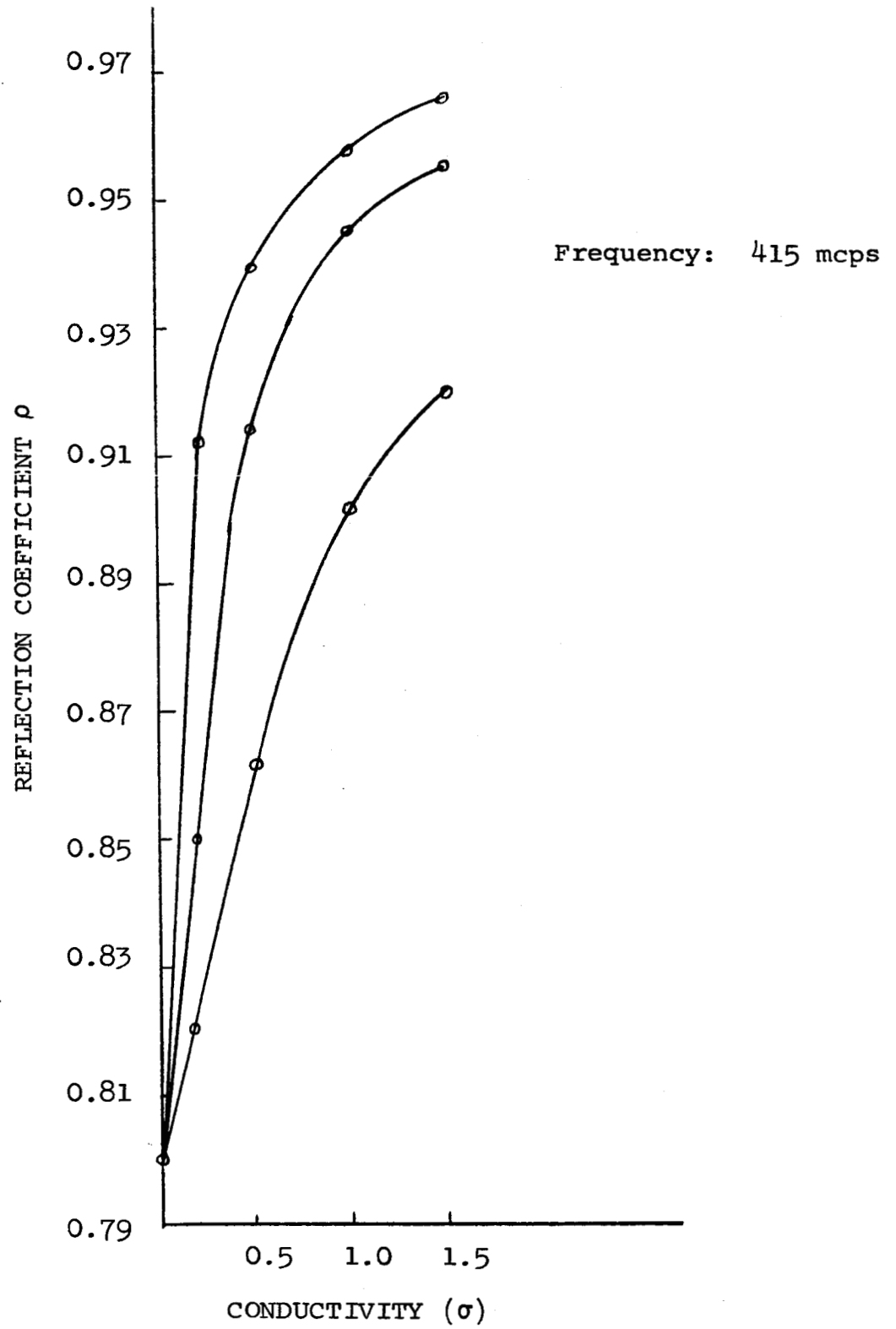
Fig. A.3 Reflection
Coefficient
Versus
Conductivity
Characteristic

Frequency = 3800 mcps

Reflection Coefficient Versus Conductivity Characteristics
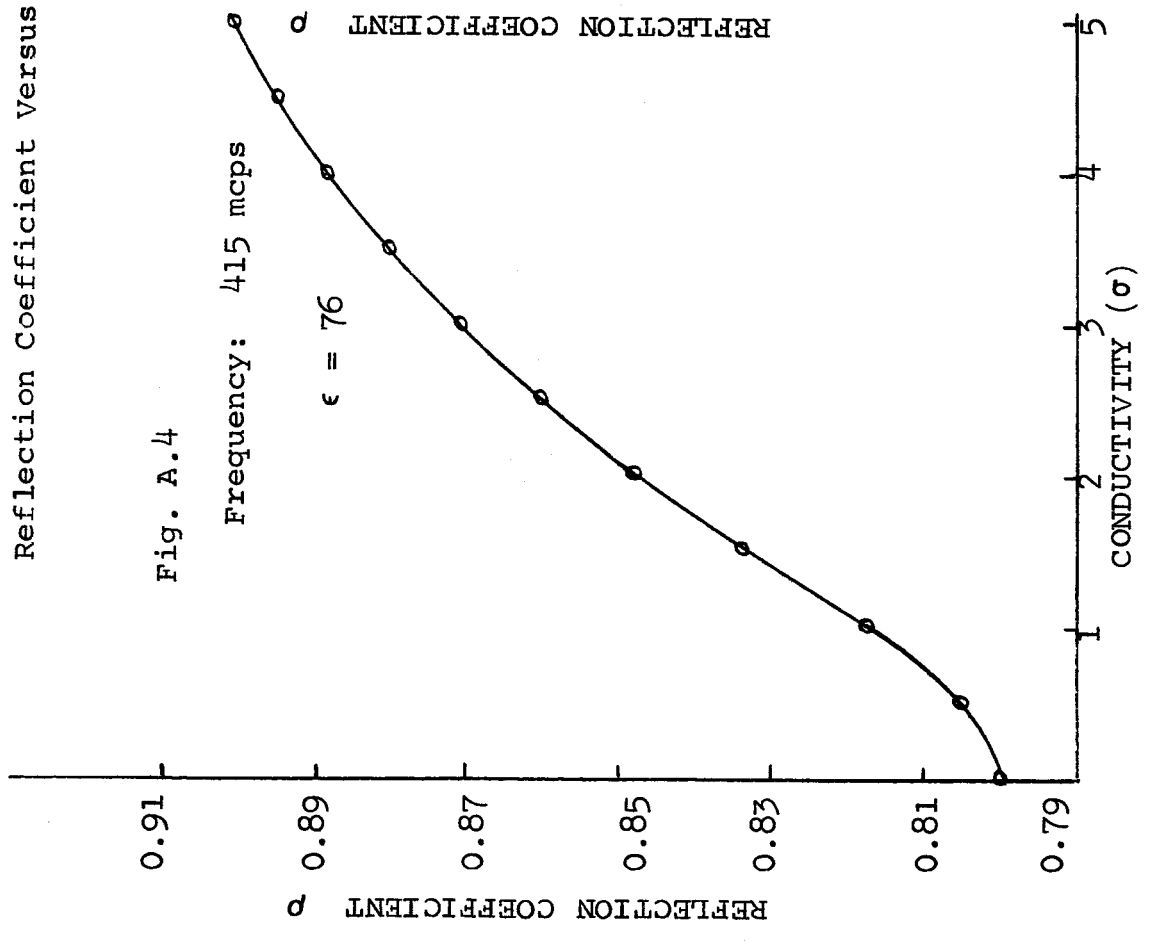
Fig. A.4

Frequency: 415 mcps

$\epsilon = 76$

Fig. A.5

Frequency: 3800 mcps

$\epsilon = 76$